P-ISSN 2586-9000
E-ISSN 2586-9027
Homepage : *https://tci-thaijo.org/index.php/SciTechAsia* Science & Technology Asia
Vol. 29 No.3 July – September 2024 Page: [214-223]
Original research article

Capacity of Decomposed Methylene Blue and Anticancer Effects of Silver Nanoparticles Using Perilla Leaf Extract

Hiep Phu Hoang, Hieu Duc Doan, Nguyet Anh Chu, Hue Thi Do*

Thai Nguyen University of Education, Thai Nguyen City 25000, Viet Nam

Received 5 December 2023; Received in revised form 22 April 2024
Accepted 23 May 2024; Available online 25 September 2024

ABSTRACT

Silver nanoparticles (AgNPs) are one of the materials with a lot of potential because of their diverse applications. AgNPs are synthesized in a variety of ways; however, with the direction of anticancer applications and decomposition of organic dyes in dyeing wastewater, AgNPs synthesized by the green method are preferred. In this study, AgNPs were synthesized using *Perilla frutescens (L.) Britt* extract called P. AgNPs. The *Perilla frutescens (L.) Britt* extract was utilized as both a surface stabilizer and a reducing agent. UV-Vis absorption spectra of the P. AgNPs was analyzed to determine how particle production is affected by the extract's pH. The shape, crystalline structure, size and size distribution of P. AgNPs were studied using TEM imaging, X-ray diffraction diagram (XRD) and dynamic light scattering (DLS). Surface functional groups and atomic composition of P. AgNPs are represented on Fourier Transformation InfraRed spectrum (FTIR) and Energy-dispersive X-ray spectroscopy (EDX). The obtained P. AgNPs are relatively uniform with an average diameter of 30 nm ± 5 nm and well distributed in the solution. P. AgNPs were deposited on activated carbon (P. AgNP- AC). P. AgNPs- AC was used to decompose methylene blue (MB) dye in the presence of H_2O_2, achieving a decomposition efficiency of up to 98. 4%. The extract or P. AgNPs exhibited potential antiproliferative activity against MDA-MB-231, HT29, and K562 cells. Interestingly, the anticancer effect of P. AgNPs was up to 2.0 times stronger than that of the leaf extract.

Keywords: Anticancer; Decompose; MB; *Perilla frutescens (L.) Britt*; Silver nanoparticles (AgNPs)

1. Introduction

Perilla's scientific name is *Perilla frutescens (L.) Britt* and it is one of the herbs friendly to human health. Leaves can be used to relieve symptoms of fever and vomiting [1]. The stem and twigs can be used to treat chest pain and bloating while the seeds are used to treat cough [2]. Furthermore, *Perilla*

***Corresponding author:** huedt@tnue.edu.vn **doi:** 10.14456/scitechasia.2024.57

frutescens (L.) Britt extracts are widely used in pharmaceuticals and cosmetics [3]. The reason *Perilla frutescens (L.) Britt* is so popular is the presence of bioactive compounds including essential oils (0.5 %, mainly perillaldehyde, l-perilla alcohol, limonene), flavonoids (quercetin, luteolin, apigenin, scutellarin), phenolic acids (caffeic, ferulic, rosmarinic acid), triterpenoids (oleanolic acid, ursolic acid, tormentic acid, corosolic acid), phytosterols (β-sitosterol, stigmasterol, campesterol), and vitamin E. [3-5].

Many studies show that the components of *Perilla frutescens (L.) Britt* leaves can be used in the synthesis of metal nanoparticles such as gold and silver nanoparticles by the biological reduction method [2, 6, 7]. The synthesis of silver nanoparticles (AgNPs) using green chemistry has been increasingly noticed, especially in research related to biomedical applications because of its environmental friendliness. Green tea leaf extract was used to synthesize AgNPs with an average diameter of about 15-33 nm and was used to test antibacterial properties against *Staphylococcus aureus* and Klebsiella bacteria [8-11]. N.S. Alharbi et al. have reviewed the use of medicinal plants for the synthesis of AgNPs [6, 12-14]. AgNPs were synthesized from leaf extract of *Aesculus hippocastanum* and their tanning activity was studied [15, 16]. The synthesis of AgNPs using the leaf extract of *Holoptelea Integrifolia* as well as its anti-inflammatory, antioxidant and catalytic activities, has also been studied [16, 17]. AgNPs with small sizes from 1 to 5 nm were synthesized using fruit extract of *Piper retrofractum*, which showed antibacterial activity against *Escherichia coli* and *S. aureus* [18-20]. Further, AgNPs with a face centered cubic crystal structure were synthesized using perilla leaf extract. However, the synthesized particles came in many different shapes such as spheres, rods, triangles, and orthorhombic geometry [7, 21].

There have been many methods used to synthesize AgNPs from plant extracts, but most AgNPs do not have a uniform size or shape. *Perilla frutescens (L.) Britt* extract with a silver nitrate solution has been used to synthesize silver nanoparticles [7]. These AgNPs showed significant anticancer activity against human colon cancer (COLO205) and prostate adenocarcinoma (LNCaP) with IC50 values of 24.33 μg/mL (for LNCaP) and 39.28 μg/mL (for COLO-205). The AgNPs exhibited apoptotic effects on LNCaP cells including cell shrinkage, membrane blebbing, chromatin condensation, fragmentation of nuclei, and formation of apoptotic bodies [7]. Silver nanoparticles synthesized with the flavonoid extract of *P. frutescens* showed cytotoxic effects against cancer cell lines including human colon carcinoma (COLO205) and mouse melanoma (B16F10), with IC50s of 59.57 and 69.33 μg/mL, respectively [22]. Silver nanoparticles made with *Perilla frutescens (L.)* extract (Pf-AgNPs) and *Perilla frutescens (L.)* extract alone also exhibited moderate toxicity on MCF-7 cancer cells with IC50 values of 346.2 and 467.4 μg/mL, respectively [23].

In this study, P.AgNPs with high efficiency and concentrated size distribution were synthesized using *Perilla frutescens (L.) Britt* extract with suitable pH. Another improvement to the nanoparticles found in this report was the deposition of the AgNPs onto activated carbon to create a photocatalytic material that can decompose MB dye with high efficiency. At the same time, the anti-cancer activity of the extract and P.AgNPs was conducted on three cell lines: *A549* (human lung carcinoma), *MDA-MB-231* (human breast carcinoma), and *K562* (human chronic myelogenous leukemia), with Ellipticine used as the positive control.

2. Materials And Methods

2.1 Materials

Perilla frutescens (L.) Britt leaves were collected in the experimental garden of

Thai Nguyen University of Education. $AgNO_3$ (99 %), activated carbon, NaOH (99%) and HCl (37-38 %) were provided by Merck. Methylene blue ($C_{16}H_{18}ClN_3S$ - MB, 98+ %), A549 cells, MDA-MB-231 cells, K562 cells and Ellipticine were provided by Sigma-Aldrich. All chemicals were used without further purification.

2.2 Methods

The method of synthesizing P.AgNPs from *Perilla frutescens (L.) Britt* extract was carried out according to a previous study [7] with some minor changes. Perilla leaves were washed several times with double distilled water to remove dust particles. The leaves were then washed with deionized water and crushed using a blender with the ratio of 10 g leaves:100 ml water. The solution obtained after grinding was filtered with a 0.2 µm pore diameter filter to remove residues. The obtained extract was stored in a refrigerator at 4°C for use in the synthesis of AgNPs. The pH of the extract was adjusted by adding 1 M NaOH or 2 M HCl such that the extract solutions had pH values ranging from 4 to 8. Subsequently, 60 ml of 1 mM $AgNO_3$ solution was added to 5 ml of the extract. The solution mixture was stirred at 500 rpm and heated at 50°C for 30 min. The color of the solution gradually changed from dark green to blue-white. The obtained products are the silver nanoparticles (P.AgNPs).

P.AgNPs were deposited on activated carbon according to the method from Wibawa [24] with slight modifications as follows: 50 ml of P.AgNPs fresh solution was mixed with activated carbon (5 g) in a 100 ml flask under magnetic stirring for up to 10 h to allow the P. AgNPs to deposit on the activated carbon to form P.AgNP-AC. The solution was then centrifuged to remove unbound substances and redispersed in double distilled water.

2.3 Application

In the photocatalysis application, 2 ml of P.AgNPs -AC solution was added to 100 ml of 10 ppm MB solution and magnetically stirred in the dark for 2 h to equilibrate the absorption. Then, the solution was illuminated with a white LED light from a 6500 K, 50 W color temperature source in the presence or absence of H_2O_2 (30 %). Degradation of the MB dye was measured by monitoring the absorption spectrum over time of illumination. The results were compared with the absence of P.AgNPs-AC to evaluate the photocatalytic performance.

Concerning the anticancer activity, the method for determining cytotoxicity used layered cultured cells following the method from a previous study [22]. As previously mentioned, the three cell lines used in this study were the A549 cell line (human lung carcinoma), the MDA-MB-231 cell line (human breast carcinoma), and the K562 cell line (human chronic myelogenous leukemia). Ellipticine served as the positive control. All treatments were performed in triplicate. The inhibition concentration 50 (IC50) value is defined as the concentration of a compound that inhibited 50% of the cell growth. The IC50 value was determined using linear regression analysis.

3. Results and Discussion

The UV-Vis absorption spectra of the extract and all the P.AgNPs formulations are presented in Fig. 1a. *Perilla frutescens (L.) Britt* extract has high absorption in the ultraviolet region while the absorption spectra of P.AgNPs have a characteristic absorption peak in the visible light region. The synthesis of P.AgNPs is strongly dependent on the pH of the extract. When the pH of the extract is below 5, the absorption spectrum is a wide band with low absorbance in the visible region and high in the UV region. This shows that the particle synthesis efficiency is lower at low pH. The UV-Vis absorption spectrum of the solution has the narrowest half-width with a maximum absorbance of 1.65 at 450 nm at pH 7. The color of the extract and of the seed solution is also shown in Fig. 1b.

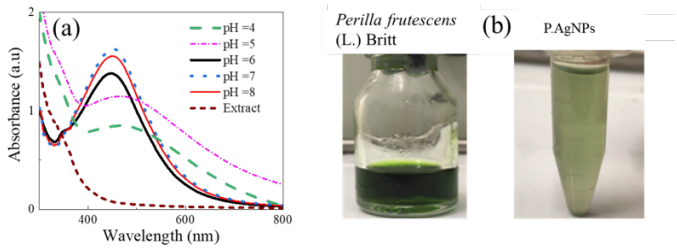

Fig. 1. UV-Vis absorption spectrum of *Perilla frutescens (L.) Britt* extract and P.AgNPs synthesized with different pH of extracts (a), images of the solutions obtain *Perilla frutescens (L.) Britt* extract and P.AgNPs (b).

The TEM images of the P.AgNPs-AC in Fig. 2a show that the particles have a relatively uniform size, with an average diameter of 30 nm ± 5 nm. The particle size distribution was determined by DLS measurement with a PdI of 0.272, indicating an average hydrodynamic diameter of 40 nm (Fig. 2b). This result shows that P.AgNPs-AC have uniformity in shape and size comparable to the chemical reduction method without using surfactants.

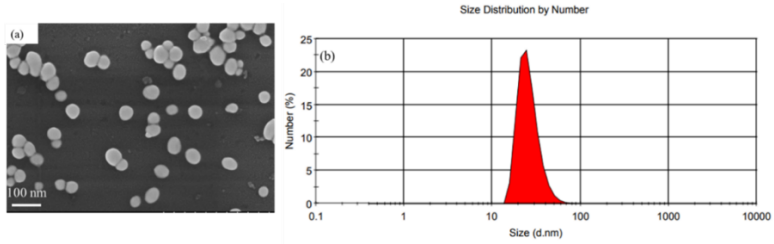

Fig. 2. TEM images of P.AgNPs - AC scale bar is 100 nm (a) and the particle size distribution spectrum by the number of particles (b).

X-ray diffraction patterns of the P.AgNPs synthesized with extract pH 6, 7, and 8 have diffraction peaks at 2θ angles of 27.5°, 32.3°, 38.1°, 44.1°, 46.3°, 64.1°, and 77.4° which correspond to the silver lattice planes (210), (122), (111), (200), (103), (220), and (311) (Fig. 3a) (JCPDS 361451). This indicates that P.AgNPs have a face centered cubic crystal structure similar to the natural structure of silver. It is noted that most of the diffraction peaks of pH 7 P.AgNPs have higher relative intensity than those of pH 6 and pH8 P.AgNPs. Fig. 3b shows the energy dispersion spectrum and element composition table obtained from EDX measurement. In addition to the elements C, Si, and O, present due to the contribution of the measurement technique, Ag is the major component of the particle sample with a dispersion peak of 3 keV.

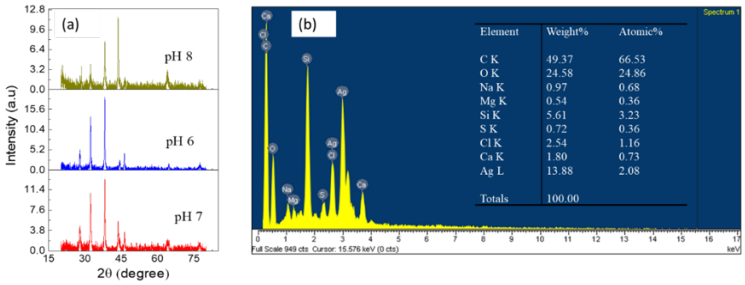

Fig. 3. X-ray diffraction of P.AgNPs synthesized with different pH extracts (a) and EDX energy dispersive spectrum of P.AgNPs (b).

The characteristic functional groups of *Perilla frutescens (L.) Britt* extract and P.AgNPs were recorded on the FTIR spectra (Fig. 4). The characteristic functional groups of *Perilla frutescens (L.) Britt* extract and P.AgNPs are basically the same. For example, the absorption peak at 1048 cm^{-1} is attributed to C-O group stretching oscillations of aromatic compounds [7]. The oscillations of the hydroxyl group of flavonoids, triterpenoids, and phenolic compounds are shown as a high-intensity wide absorption band at 3310 cm^{-1} [7]. The slight shift at some positions between the FTIR spectrum of *Perilla frutescens (L.) Britt* extract and that of P.AgNPs can be explained by the effects of proteins, which cap around the P. AgNPs surface and act as stabilizing agents. This allows the P.AgNPs to remain stable in solution without agglomeration.

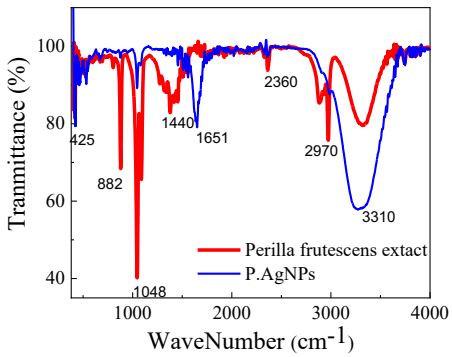

Fig. 4. FTIR spectra of *Perilla frutescens (L.) Britt* extract and P.AgNPs with some characteristic peaks.

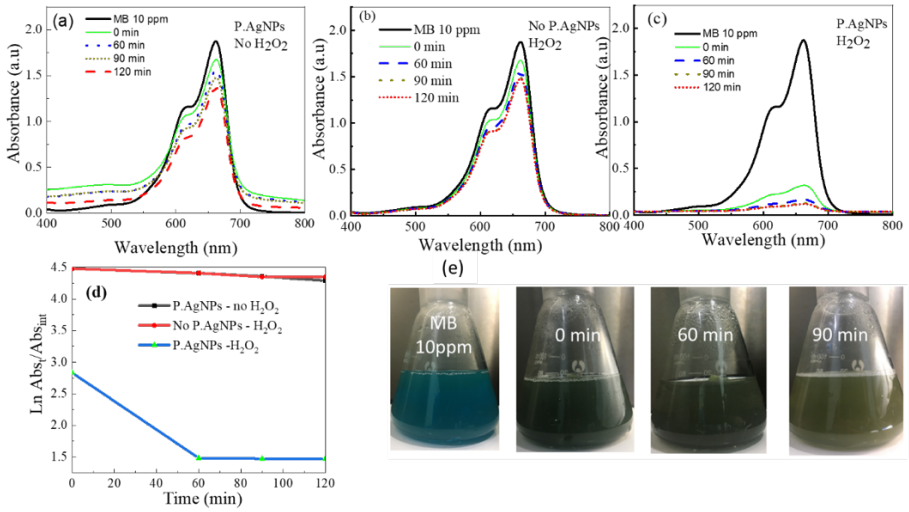

Fig. 5. UV-Vis absorption spectra of MB dye under 6500 K LED excitation over time in the presence of P.AgNPs-AC and no H_2O_2 (a), No P.AgNPs-AC and H_2O_2 (b), P.AgNPS-AC and H_2O_2 (c). Photograph of the color change of solutions when illuminated in the presence of P.AgNPs-AC and H_2O_2 over time (e).

P.AgNPs-AC were used to study the photocatalytic activity on MB dye degradation under the excitation of white light from a 30W LED, with a color temperature of 6500 K. This light source has a wavelength above 400 nm, with a peak wave of 464 nm. Photodegradation is represented by a decrease in absorbance of MB with increasing time of illumination. To observe the catalytic role of P.AgNPs-AC, the

experiments were designed including a solution containing only H_2O_2 reducing agent as reference [24] a solution containing only P.AgNPs-AC, and a solution containing both P.AgNPs -AC and H_2O_2. The absorbance of MB over time is shown in Fig. 5.

The absorbance of initial 10 ppm MB was 1.9. After 120 min of illumination, the absorbance decreased to 1.33 (only P.AgNPs -AC-Fig. 5a), 1.51 (only H_2O_2-Fig. 5b) and 0.03 (P.AgNPs-AC and H_2O_2-Fig. 5c). The photodegradation efficiency was determined by the formula: $H = [(Ab_{Int} - Abs_t) / Abs_{Int}] \times 100\%$, where Abs_{Int} is the initial MB absorption, Abs_t is the MB absorption after illumination for time *t.* This decrease in absorbance is equivalent to MB absorption efficiency. Results showed photodegradation efficiencies of 30% (only P.AgNPs-AC), 20.5% (only H_2O_2), and 98.4% (P.AgNPs -AC and H_2O_2). There were both P.AgNPs -AC and H_2O_2 in the solution; as soon as the solution reached equilibrium, the absorbance of MB in the solution decreased significantly. This is explained by the strong adsorption of color molecules by AgNPs with the assistance of H_2O_2 reducing agent. However, there will then be a desorption process if there is no light stimulation. Under the influence of light, the colorant decomposition process continues thanks to the formation of free $^*OH$ groups. The dependence of the $\ln(Abs_t/Abs_{Int})$ function on illumination time is shown in Figure 5d. The results show that when only AgNPs or only H_2O_2 is present, the color molecules are decomposed equally. Decomposition quickly reaches saturation at which point no further decomposition is possible. In the presence of AgNPs and H_2O_2 simultaneously, MB was almost completely decomposed after 60 min. The photocatalytic mechanism of P.AgNPs-AC can be briefly mentioned as follows: The photocatalytic effect depends on the production of electron-hole pairs which generate $^*OH$ radicals [25, 26].

$$\text{P. AgNPs -AC} + h\nu \rightarrow \text{P.AgNPs (h + e)} \quad (3.1)$$

$$h + H_2O \rightarrow H^+ + {}^*OH \quad (3.2)$$

$$H_2O_2 + h\nu \rightarrow {}^*OH + {}^*OH \quad (3.3)$$

$$MB + {}^*OH + O_2 \rightarrow H_2O + CO_2 + \text{byproducts} \quad (3.4)$$

Thus, it can be seen that the h hole and the $^*OH$ free radical are the direct color-degrading agents when using P.AgNPs-AC under light stimulation. The simultaneous presence of the reducing agent H_2O_2 and AgNPs -AC during the decomposition of the dye significantly increased the number of $^*OH$ groups. On the other hand, the decomposition is facilitated by the transfer of electrons from H_2O_2 to MB dye via AgNPs, which creates an electron-rich surface for the interaction between reactants and can aid in the attraction of dye molecules onto the AgNPs surface through hydrophobic interactions and van der Waals forces.

Based on the linear regression equations, IC50 values for the cancer cell lines were calculated (Table 1).

Table 1. Inhibitory activity (IC50) in proliferation of cancer cell lines (μg/ml).

Sample \ Line cell	MDA-MB-231 cell	HT29 cell	K562 cell
Perilla extract	22.48	24.50	21.20
P.AgNPs	11.40	13.00	11.68
Ellipticine	0.42	0.40	0.42

The results show that the percentage of dead cells in MDA-MB-231, HT29, and K562 cell lines is influenced by the concentration of the extract or nanoparticles. Increased concentration led to a higher percentage of dead cells in all cell lines (Fig 6). These findings suggest that the extract or nanoparticles of perilla leaves exhibit potential antiproliferative activity against MDA-MB-231, K562 and HT29 cells. Notably, P.AgNPs activity was up to 2.0 times more potent than the leaf extract alone. Among the cell lines, MDA-MB-231 experienced the greatest inhibitory effect on growth (11.40 μg/ml), while the HT29 cells were the least effected (13.00 μg/ml).

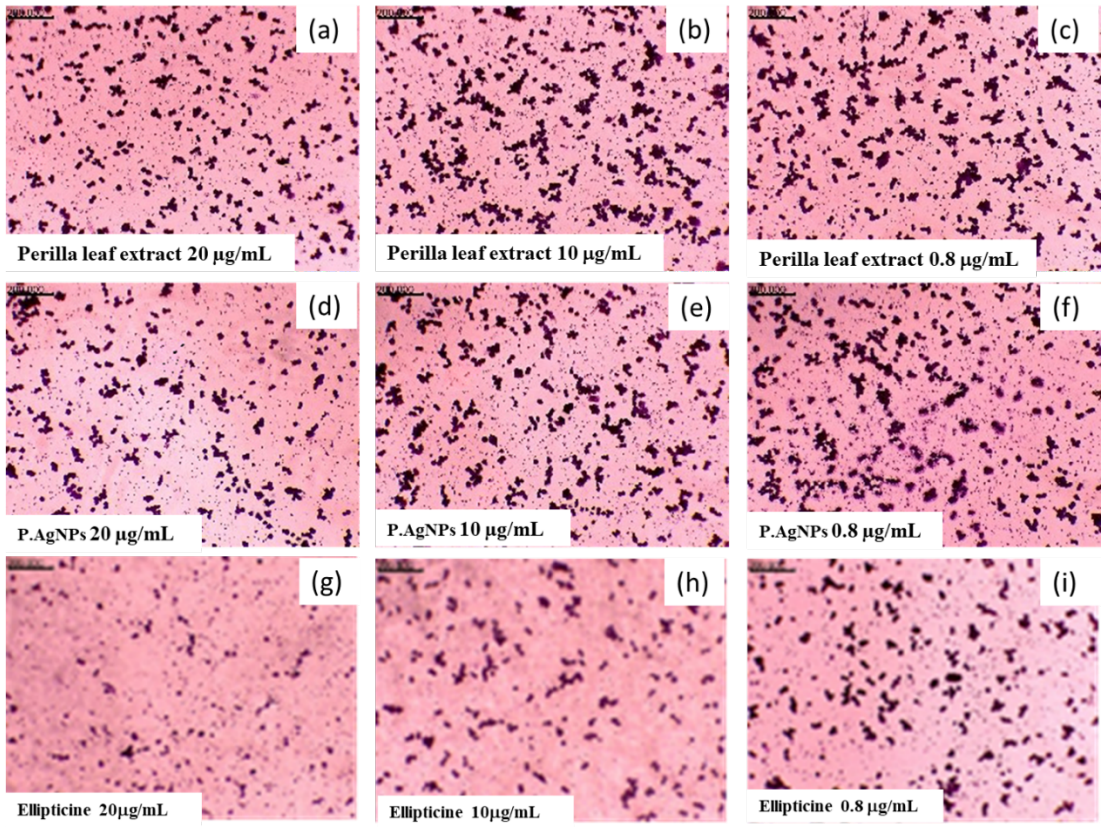

Fig. 6. Anticancer activity of the *Perilla frutescens (L.) Britt* extract, P.AgNPs and Ellipticine (positive control) in various concentrations against HT-29 cancer cell line. Morphological images were taken using an inverted phase-contrast microscope at 200X magnification.

The *Perilla frutescens (L.) Britt* essential oil have some major bioactive components such as: perillyl alcohol, perilla aldehyde, rosmarinic acid, lignan, isoestrogen, limonene, linalool, caryophyllene, humulene, cineole, ocimen, eugenol, alpha-pinene, myrcene, and more. These compounds can effect cell growth, proliferation, inflammation, cell cycle, apoptosis, and metastasis through ROS, NF-κB, PI3K/AKT, JNK, and other pathways [27].

Concerning cytotoxicity, *Perilla frutescens (L.) Britt* essential oil, particularly its major component perillyl alcohol, exhibits direct cytotoxicity towards cancer cells. One possible explanation for this is that Perillyl alcohol interacts with the cell membrane, leading to increased permeability and leakage of essential cellular components, ultimately causing cell death [28].Another explanation could be that the oil triggers programmed cell death pathways within cancer cells, leading to their self-destruction [29]. A third explanation, Perillyl alcohol can arrest the cell cycle at various stages, preventing cancer cells from multiplying [30]. For anti-proliferative effects, the essential oil suppresses uncontrolled growth and proliferation of cancer cells through various mechanisms, including downregulating oncogenes and upregulating tumor suppressor genes [31]. Green nanotechnology-derived metal nanoparticles are emerging as versatile players in cancer treatment and research, captivating interest due to their biocompatibility, cost-effectiveness, eco-friendliness, and anticancer properties [32].

4. Conclusion

In this study, P.AgNPs were synthesized using *Perilla frutescens (L.) Britt* extract. The reaction yield was optimized by adjusting the pH of the extract. The results show that with a neutral pH medium, P.AgNPs are more uniform in shape and size. The silver nanoparticles synthesized from *Perilla frutescens (L.) Britt* extract are well dispersed and stable in solution due to the phenolic compounds and proteins present in the extract. Furthermore, P.AgNPs synthesized using plant extracts are environmentally friendly and are useful in more applications. P. AgNPs-AC were used to study the photocatalytic activity of MB dye. The results show that under the excitation of white light and the presence of H_2O_2 and P.AgNPs-AC, the MB dye decomposition efficiency can go up to 98.4 % after just 90 min. This result is much better than when using only H_2O_2 or using only P.AgNPs-AC. P. AgNPs and perilla were used to study anticancer activity on three cancer cell lines. The results show that both the extract and P.AgNPs have anti-cancer activity in vitro. The activity becomes stronger the greater the extract or particle concentration. P.AgNPs showed 2.0 times stronger activity than the extract and were different for different cell lines. The IC50 value depended on concentration, particle size of P.AgNPs and cell line.

Acknowledgements

The authors would like to thank TNU for providing equipment to complete the project code ĐH2023-TN04-06.

References

[1] Asif M. Health effects of omega-3,6,9 fatty acids: Perilla frutescens is a good example of plant oils. Orient Pharm Exp Med. 2011 Mar;11(1):51-9.

[2] Adam G, Robu S, Flutur MM, Cioanca O, Vasilache IA, Adam AM, et al. Applications of Perilla frutescens Extracts in Clinical Practice. Vol. 12, Antioxidants. MDPI; 2023.

[3] Dhyani A, Chopra R, Garg M. A review on nutritional value, functional properties and pharmacological application of perilla (Perilla frutescens L.). Biomedical and Pharmacology Journal. 2019;12(2):649-60.

[4] Bachheti RK, Archana Joshi, Tofik Ahmed, A Phytopharmacological Overview on Perilla frutescens, Int. J. Pharm. Sci. Rev. Res., 26(2), May - Jun 2014; Article No. 11, Pages: 55-61.

[5] Rehan S, Mazumdar AH, Shamsi IA, Karmakar S, Rehan AS, Alam SI, et al. A systematic review on multi-nutritional and phytopharmacological importance of Perilla frutescens Medicinal Plants of Northeast States of India as Potential Therapies for Malaria View project Application of Nanoprotein in Food Industry and Its Potential Toxicity related Health Issues View project A systematic review on multi-nutritional and phytopharmacological importance of Perilla frutescens. Vol. 16, International Journal of Green Pharmacy. Available from: https://www.researchgate.net/-publication/364027364.

[6] Alharbi NS, Alsubhi NS, Felimban AI. Green synthesis of silver nanoparticles using medicinal plants: Characterization and application. J Radiat Res Appl Sci. 2022 Sep;15(3):109-24.

[7] Reddy N V., Li H, Hou T, Bethu MS, Ren Z, Zhang Z. Phytosynthesis of silver nanoparticles using perilla frutescens leaf extract: Characterization and evaluation of antibacterial, antioxidant, and anticancer activities. Int J Nanomedicine. 2021;16:15-29.

[8] Widatalla HA, Yassin LF, Alrasheid AA, Rahman Ahmed SA, Widdatallah MO, Eltilib SH, et al. Green synthesis of silver nanoparticles using green tea leaf extract, characterization and evaluation of

antimicrobial activity. Nanoscale Adv. 2022 Feb 7;4(3):911-5.

[9] Nakhjavani M, Nikkhah V, Sarafraz MM, Shoja S, Sarafraz M. Green synthesis of silver nanoparticles using green tea leaves: Experimental study on the morphological, rheological and antibacterial behaviour. Heat and Mass Transfer/Waerme- und Stoffuebertragung. 2017 Oct 1;53(10):3201-9.

[10] Iqra, Khattak R, Begum B, Qazi RA, Gul H, Khan MS, et al. Green Synthesis of Silver Oxide Microparticles Using Green Tea Leaves Extract for an Efficient Removal of Malachite Green from Water: Synergistic Effect of Persulfate. Catalysts. 2023 Feb 1;13(2).

[11] Kalakonda P, Kumar Debbeta N, Kathi R, Kishan Manduri G, Kumar Bathula N, Jadi B, et al. Facile Synthesis of Silver Nanoparticles using Green Tea Leaf extract and Evolution of Antibacterial activity.

[12] Habeeb Rahuman HB, Dhandapani R, Narayanan S, Palanivel V, Paramasivam R, Subbarayalu R, et al. Medicinal plants mediated the green synthesis of silver nanoparticles and their biomedical applications. Vol. 16, IET Nanobiotechnology. John Wiley and Sons Inc; 2022. p. 115-44.

[13] Ajaykumar AP, Mathew A, Chandni AP, Varma SR, Jayaraj KN, Sabira O, et al. Green Synthesis of Silver Nanoparticles Using the Leaf Extract of the Medicinal Plant, Uvaria narum and Its Antibacterial, Antiangiogenic, Anticancer and Catalytic Properties. Antibiotics. 2023 Mar 1;12(3).

[14] Shah MZ, Guan ZH, Din AU, Ali A, Rehman AU, Jan K, et al. Synthesis of silver nanoparticles using Plantago lanceolata extract and assessing their antibacterial and antioxidant activities. Sci Rep. 2021 Dec 1;11(1).

[15] Riaz M, Suleman A, Ahmad P, Khandaker MU, Alqahtani A, Bradley DA, et al. Biogenic Synthesis of AgNPs Using Aqueous Bark Extract of Aesculus indica for Antioxidant and Antimicrobial Applications. Crystals (Basel). 2022 Feb 1;12(2).

[16] Küp FÖ, Çoşkunçay S, Duman F. Biosynthesis of silver nanoparticles using leaf extract of Aesculus hippocastanum (horse chestnut): Evaluation of their antibacterial, antioxidant and drug release system activities. Materials Science and Engineering C. 2020 Feb 1;107.

[17] Kumar V, Singh S, Srivastava B, Bhadouria R, Singh R. Green synthesis of silver nanoparticles using leaf extract of Holoptelea integrifolia and preliminary investigation of its antioxidant, anti-inflammatory, antidiabetic and antibacterial activities. J Environ Chem Eng. 2019 Jun 1;7(3).

[18] Amaliyah S, Sabarudin A, Masruri M, Sumitro SB. Characterization and antibacterial application of biosynthesized silver nanoparticles using Piper retrofractum Vahl fruit extract as bioreductor. J Appl Pharm Sci. 2022 Mar 1;12(3):103-14.

[19] Amaliyah S, Masruri M, Sabarudin A, Sumitro SB. Sonication-assisted green synthesis of silver nanoparticles using Piper retrofractum fruit extract and their antimicrobial assay. In: AIP Conference Proceedings. American Institute of Physics Inc.; 2021.

[20] Santhoshkumar R, Hima Parvathy A, Soniya E V. Phytosynthesis of silver nanoparticles from aqueous leaf extracts of Piper colubrinum: characterisation and catalytic activity. J Exp Nanosci. 2021;16(1):295-309.

[21] Basavegowda N, Lee YR. Synthesis of gold and silver nanoparticles using leaf extract of perilla frutescens - A biogenic approach. J Nanosci Nanotechnol. 2014;14(6):4377-82.

[22] Hou T, Guo Y, Han W, Zhou Y, Netala VR, Li H, et al. Exploring the Biomedical Applications of Biosynthesized Silver Nanoparticles Using Perilla frutescens Flavonoid Extract: Antibacterial, Antioxidant, and Cell Toxicity Properties against Colon Cancer Cells. Molecules. 2023 Sep 1;28(17).

[23] Tavan M, Hanachi P, Mirjalili MH, Dashtbani-Roozbehani A. Comparative assessment of the biological activity of the green synthesized silver nanoparticles and aqueous leaf extract of Perilla frutescens (L.). Sci Rep. 2023 Dec 1;13(1).

[24] Taha A, Aissa M Ben, Da'na E. Green synthesis of an activated carbon-supported Ag and ZnO nanocomposite for photocatalytic degradation and its antibacterial activities. Molecules. 2020;25(7).

[25] Madhu, Sharma R, Bharti R. A Review on the Synthesis and Photocatalytic Application of Silver Nano Particles. In: IOP Conference Series: Earth and Environmental Science. Institute of Physics; 2023.

[26] Kadam J, Dhawal P, Barve S, Kakodkar S. Green synthesis of silver nanoparticles using cauliflower waste and their multifaceted applications in photocatalytic degradation of methylene blue dye and Hg2+ biosensing. SN Appl Sci. 2020 Apr 1;2(4).

[27] Huang S, Nan Y, Chen G, Ning N, Du Y, Lu D, et al. The Role and Mechanism of Perilla frutescens in Cancer Treatment. Vol. 28, Molecules. Multidisciplinary Digital Publishing Institute (MDPI); 2023.

[28] Kong H, Zhou B, Hu X, Wang X, Wang M. Protective effect of Perilla (Perilla frutescens) leaf essential oil on the quality of a surimi-based food. J Food Process Preserv. 2018 Mar 1;42(3).

[29] Wang R, Zhang Q, Feng C, Zhang J, Qin Y, Meng L. Advances in the Pharmacological Activities and Effects of Perilla Ketone and Isoegomaketone. Vol. 2022, Evidence-based Complementary and Alternative Medicine. Hindawi Limited; 2022.

[30] Abd El-Hafeez AA, Fujimura T, Kamei R, Hirakawa N, Baba K, Ono K, et al. A methoxyflavanone derivative from the Asian medicinal herb (Perilla frutescens) induces p53-mediated G2/M cell cycle arrest and apoptosis in A549 human lung adenocarcinoma. Cytotechnology. 2018 Jun 1;70(3):899-912.

[31] Wang Y, Huang X, Han J, Zheng W, Ma W. Extract of Perilla frutescens inhibits tumor proliferation of HCC via PI3K/AKT signal pathway. African journal of traditional, complementary, and alternative medicines : AJTCAM / African Networks on Ethnomedicines. 2013;10(2):251-7.

[32] Mbatha LS, Akinyelu J, Chukwuma CI, Mokoena MP, Kudanga T. Current Trends and Prospects for Application of Green Synthesized Metal Nanoparticles in Cancer and COVID-19 Therapies. Vol. 15, Viruses. MDPI; 2023.